Full citation: Yu-Kai Lin, Wen-Chieh Lin, and Chieh-Chih Wang, "K-Closest Points and Maximum Clique Pruning for Efficient and Effective 3-D Laser Scan Matching," *IEEE Robotics and Automation Letters (RA-L)*, vol. 7, no. 2, pp. 1471–1477, Apr. 2022. DOI: 10.1109/LRA.2021.3140130.

K-Closest Points and Maximum Clique Pruning for Efficient and Effective 3-D Laser Scan Matching

Yu-Kai Lin[1], Wen-Chieh Lin[1], and Chieh-Chih Wang[2]

***Abstract*—We propose K-Closest Points (KCP), an efficient and effective laser scan matching approach inspired by LOAM and TEASER++. The efficiency of KCP comes from a feature point extraction approach utilizing the multi-scale curvature and a heuristic matching method based on the k-closest points. The effectiveness of KCP comes from the integration of the feature point matching approach and the maximum clique pruning. We compare KCP against well-known scan matching approaches on synthetic and real-world LiDAR data (nuScenes dataset). In the synthetic data experiment, KCP-TEASER reaches a state-of-the-art root-mean-square transformation error $(0.006\text{m}, 0.014^\circ)$ with average computational time 49ms. In the real-world data experiment, KCP-TEASER achieves an average error of $(0.018\text{m}, 0.101^\circ)$ with average computational time 77ms. This shows its efficiency and effectiveness in real-world scenarios. Through theoretic derivation and empirical experiments, we also reveal the outlier correspondence penetration issue of the maximum clique pruning that it may still contain outlier correspondences.**

***Index Terms*—Range Sensing, Mapping, Computer Vision for Transportation**

I. Introduction

POINT clouds registration is a fundamental problem in many applications of robotics, computer vision, and computer graphics. In autonomous driving, point cloud registration or scan matching is commonly used to find the relative pose transformation between two consecutive scans. With recent advances in range sensors, LiDARs have been one of the the preferred sensing options in autonomous driving due to their reliability and stability. However, LiDAR scans are often distorted and affected by noise in real-world scenarios. Therefore, fast and accurate point cloud registration based on LiDAR measurements is highly demanded [1], [2].

The registration problem has a closed-form least squares solution obtained by the singular value decomposition if a set of ground truth correspondences is given. However, the correspondence set is usually unknown in most real-world cases. Thus, there are many methods dedicated to handle the correspondence problem, such as estimating pose and correspondences simultaneously [3], [4], reducing the dependencies of the correspondence set [5], [6], or filtering out incorrect correspondences through geometric constraints [7]–[9].

A fast and robust approach for feature-based point cloud registration, Truncated least squares Estimation And SEmidefinite Relaxation (TEASER++) [8], was proposed recently. For applications of object pose estimation and scan matching, TEASER++ utilized two matching methods to establish the feature correspondences, 3DSmoothNet [10] and Fast Point Feature Histograms (FPFH) [11], respectively. However, the matching approach of 3DSmoothNet [10] requires high computational cost when calculating the voxelized smoothed density value representation. On the other hand, the matching

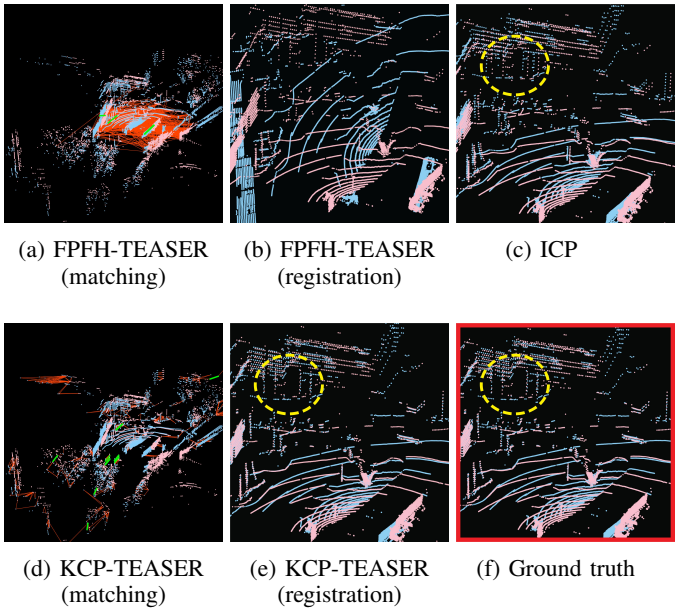

(a) FPFH-TEASER (matching) (b) FPFH-TEASER (registration) (c) ICP

(d) KCP-TEASER (matching) (e) KCP-TEASER (registration) (f) Ground truth

Fig. 1: Point cloud registration results of FPFH-based TEASER++ (FPFH-TEASER), ICP, and KCP-TEASER on real-world LiDAR scans. Two point clouds scanned at different times are displayed in blue and pink colors. Estimated inlier and outlier correspondences are represented by red and green lines in (a) and (d). In this example, (a) The set of inlier correspondences with FPFH cannot provide clear and consistent information about matching, resulting in (b) an incorrect registration result. In contrast, (c) ICP registration with raw points successfully finds a proper transformation but converges to a local minimum. KCP-TEASER considers (d) a smaller but more consistent set of correspondences under sparse feature clouds, and computes (e) an accurate transformation close to (f) the ground truth registration.

Manuscript received: September 9, 2021; Revised November 30, 2021; Accepted December 17, 2021.

This paper was recommended for publication by Editor Sven Behnke upon evaluation of the Associate Editor and Reviewers' comments. This work was supported by the Taiwan Ministry of Science and Technology under Grants 109-2221-E-009-119-MY3 and 109-2221-E-009-120-MY3.

[1]Yu-Kai Lin and Wen-Chieh Lin are with the Institute of Multimedia Engineering, National Yang Ming Chiao Tung University, Hsinchu, Taiwan yukai.cs09g@nctu.edu.tw, wclin@cs.nctu.edu.tw

[2]Chieh-Chih Wang is with the Department of Electrical and Computer Engineering, National Yang Ming Chiao Tung University, and with the Mechanical and Mechatronics Systems Research Laboratories, Industrial Technology Research Institute, Hsinchu, Taiwan bobwang@ieee.org

Digital Object Identifier (DOI): see top of this page.

approach with FPFH may result in either a large or poor set of feature point correspondences, which is likely to produce incorrect registration results, as shown in Figures 1(a) and 1(b).

In addition, to demonstrate the ability of solving a registration problem without correspondences, TEASER++ further provides a proof-of-concept registration that considers the direct product of two point clouds as the set of correspondences. However, a large amount of correspondences fed to the maximum clique algorithm used in TEASER++ may raise an extremely huge computational cost. In fact, the maximum clique problem is derived from one of Karp's 21 NP-complete problems.

In this paper, we propose an approach to overcome the poor initial feature correspondence set and to reduce the high computational cost coming from the maximum clique algorithm. The key idea is to efficiently construct a better and smaller set of feature correspondences. To achieve the goal, our proposed method adopts an efficient algorithm to rank and extract feature points based on their reliability, as well as a neighbor-based searching approach to compute correspondences between two sets of feature points. The reliability measure is based on the multi-scale curvature, where the main idea is adopted by LOAM [12] but we modify the formulation to make the measure of curvature more accurate, and the feature matching approach using neighbor searching is called the k-closest points. This procedure ensures that the initial set of correspondences remains a small cardinality, and hence the maximum clique of the corresponding graph can be efficiently calculated to refine the set of correspondences. A relative transformation is eventually computed from the refined feature point correspondences with the solvers introduced in TEASER++, as shown in Figure 1(d) and 1(e).

The proposed method is evaluated with a synthetic and a real-world LiDAR scan matching tasks under the nuScenes dataset [13]. KCP-TEASER presents fast and accurate results in both experiments, where KCP-TEASER is on average 129 times faster than 3DSmoothNet-based TEASER++, while the root-mean-square error only increased by $(0.001\mathrm{m}, 0.003^\circ)$ in the synthetic experiment. Moreover, in the real-world experiment, transformation results of KCP-TEASER are 39% and 7% more accurate than the results of 3DSN-TEASER in terms of root-mean-square translation and rotation errors. Lastly, the ablation study within the synthetic experiment also validates the strengths of KCP.

Contributions. This work proposes an efficient and effective approach to estimate a small but accurate set of correspondences within two consecutive laser scans. Our approach greatly reduces the computational cost of the maximum clique, and reaches a state-of-the-art accuracy of rigid transformation results. In both theoretical and empirical aspects, we also point out the outlier correspondence penetration issue that some outliers could be selected in the maximum clique.

II. Related Work

A. Point Cloud Registration

Rigid registration problem can be challenging if correct correspondences are unknown. In general, the registration problems are categorized into local and global approaches according to whether they attempt to find the globally optimal transformation.

Local Registration. Local registration approaches do not consider the global optimality of the estimation. Iterative Closest Point (ICP) [3] is a classical approach that refines the set of correspondences and computes the optimal solution using Horn et al.'s method [14] iteratively. The performance of ICP relies on good initial guesses since it is easy to converge to a local minimum. Probabilistic approaches, such as Normal Distribution Transform (NDT) [5] and Generalized-ICP (GICP) [6], formulate cells or points with Gaussian distribution and register two point clouds by minimizing probability-based distance metrics to conquer some robustness issues.

Global Registration. Global registration approaches consider the problem in the entire three dimensional special Euclidean group $\mathrm{SE}(3)$ and compute the globally optimal solution of a formulated optimization problem with several types of point descriptors, such as histograms [11], eigenvalues along with normals [15], and a voxelized smoothed density value (SDV) [10]. With the rise of machine learning, several approaches, e.g., 3DFeat-Net [16] and FCGF [17], are proposed to study feature representation of points with neural networks. SKD [18] proposes a learning-based approach to extract keypoints using saliency estimation. D3Feat [19] jointly studies keypoint detection and description with a dense feature extraction network followed by a keypoint detection criterion. These approaches simply use RANSAC [20] to estimate registration results based on their computed point correspondences.

As for the progress of registration methods, Globally Optimal ICP (Go-ICP) [4] searches the solution of the registration problem globally using the paradigm of the branch-and-bound (BnB). TEASER [9] proposes a truncated least squares-based registration problem, and exploits semidefinite relaxation to transfer the rotation estimation problem into a large-scale semidefinite programming (SDP). Based on TEASER, TEASER++ [8] improves computational efficiency by solving the rotation estimation problem with the graduated non-convexity algorithm with the truncated least squares (GNC-TLS) [21], and provides an algorithm to certify the global optimality of the estimated rotation matrix. Phase Registration (PHASER) [2] deals with the point cloud registration problem using the spherical Fourier analysis that can also decouple the registration problem into the rotation and translation parts. PHASER avoids the matching issue by using spectrum so that it does not require point correspondences.

Positioning of KCP. KCP is a local registration approach since the proposed method attempts to search correspondences locally in the spatial domain. This strategy would degrade the global registration solver TEASER++ [8] to a local approach; nevertheless, it is effective to mitigate the computational complexity of the maximum clique problem, and makes the solver more suitable for use in real-world robotics scenarios. There are two major differences that distinguish our work from the approaches that inspire KCP:

1) The computational issues of complexity and outlier

correspondence penetration are rarely mentioned in TEASER [9] and TEASER++ [8]. Our work mitigates the computational complexity issue, and point out the outlier correspondence penetration issue theoretically and empirically.

2) The smoothness term in LOAM [12] is lack of the spacing concept in numerical differentiation. Our work formulates the multi-scale curvature based on the finite difference, resulting in more accurate approximation of curvature.

B. Pairwise Constraints for Shape Correspondences

Under the assumption of rigid transformation, there is a series of 0-1 integer programming problems whose solution corresponds to the set of inlier correspondences. The formulation usually relates to weighted affinity matrices [22], [23] or unweighted association graphs [7]–[9], [24], [25], where the former are usually solved with some relaxation such as spectral clustering [23], softassign technique [26], or solved directly by searching [22], and the latter are considered to be the maximum clique problem [7]–[9], [24] or the vertex cover problem [25].

III. Proposed Method

In this section, we introduce the proposed method that finds the relative rotation $\hat{R} \in \mathrm{SO}(3)$ and translation $\hat{\boldsymbol{t}} \in \mathbb{R}^3$ between the laser scan $\mathcal{X}_t = \{\boldsymbol{x}_{t,i} \in \mathbb{R}^3 : i = 1, \dots, n_t^{\mathrm{x}}\}$ at time t and its consecutive previous scan $\mathcal{X}_{t-1}$, which leads to solve the following optimization problem:

$$(\hat{R}, \hat{\boldsymbol{t}}) = \underset{R \in \mathrm{SO}(3), \boldsymbol{t} \in \mathbb{R}^3}{\arg\min} \sum_{(\boldsymbol{a}, \boldsymbol{b}) \in \mathcal{C}_{t,t-1}} \rho\left(\frac{1}{\varepsilon^2} \|\boldsymbol{b} - R\boldsymbol{a} - \boldsymbol{t}\|_2^2\right), \tag{1}$$

where $\mathcal{C}_{t,t-1} \subseteq \mathcal{X}_t \times \mathcal{X}_{t-1}$ is a set of unknown correspondences between $\mathcal{X}_t$ and $\mathcal{X}_{t-1}$, $\rho(\cdot) = \min(\cdot, 1)$ is a truncated least squares cost function, $\varepsilon \in \mathbb{R}_{>0}$ is the noise bound of measurements, and $\mathrm{SO}(3)$ is the 3D rotation group.

The architecture of KCP is shown in Figure 2. In the beginning, corner points are extracted from raw point clouds $\mathcal{X}_t$ and $\mathcal{X}_{t-1}$ using surface parametrization and discrete calculus (Section III-A). Next, a set of correspondences between two sets of feature points is constructed with a heuristic approach and graph-based pairwise constraints (Section III-B). Finally, the relative transformation with respect to the set of correspondences is computed based on Equation (1).

A. Corner Points Extraction with Multi-scale Curvatures

Curvatures of a point within a continuous parametric surface are classic and reliable measurements to describe the bending of its neighborhood. Larger curvatures usually indicate sharp corners of a surface, and the sparsity of these points makes them suitable as feature points for scan registration [27]. Therefore, we design an approximate curvature measure for 3D point clouds, and extract corner points for the forthcoming matching step. The main formulation is adopted from LOAM [12], but we modify the equation based on the finite difference.

Each scan $\mathcal{X}_t$ is first converted into a range image $\mathcal{R}_t$ using the spherical projection,

$$(\theta, \varphi) \mapsto (r \sin\varphi \cos\theta, r \sin\varphi \sin\theta, r \cos\varphi), \tag{2}$$

where $\theta \in (0, 2\pi]$ represents the horizontal field of view, $\varphi \in (0, \pi)$ represents the vertical field of view, and the spatial point described by (r, θ, φ) is considered as a point of $\mathcal{X}_t$. With mapping and discretization, there is a matrix $\mathcal{R}_t \in \mathbb{R}^{n^{\mathrm{v}} \times n^{\mathrm{h}}}$ with entry $(\mathcal{R}_t)_{ij} = r$ representing the depth of the corresponding point,

$$\left(r \sin\frac{i\pi}{n^{\mathrm{v}}} \cos\frac{2j\pi}{n^{\mathrm{h}}}, r \sin\frac{i\pi}{n^{\mathrm{v}}} \sin\frac{2j\pi}{n^{\mathrm{h}}}, r \cos\frac{i\pi}{n^{\mathrm{v}}}\right) \in X_t, \tag{3}$$

where n^{v} and n^{h} are the resolutions of vertical and horizontal fields of view (FOV).

Using the i-th row vector as the curve of a point at (i, j) in $\mathcal{R}_t$, we define the discrete curvature by

$$\kappa_{t,s}(i, j) = \frac{1}{s}\Big((\mathcal{R}_t)_{i,j+s} + (\mathcal{R}_t)_{i,j-s} - 2(\mathcal{R}_t)_{ij}\Big) \tag{4}$$

with a given spacing $s \in \mathbb{N}$ of numerical differentiation. Eventually the absolute value of mean of curvatures within n^{s} scales

$$\kappa_t(i, j) = \left|\frac{1}{n^{\mathrm{s}}} \sum_{s=1}^{n^{\mathrm{s}}} \kappa_{t,s}(i, j)\right| \tag{5}$$

is computed to be the multi-scale curvature of the vertex. This scalar descriptor of Equation (5) is similar to the smoothness term defined in LOAM [12]. However, LOAM omits the term $1/s$ in Equation (4) and in this case Equation (4) is a more accurate approximation of curvature because we define it based on the finite difference for numerical differentiation.

We extract features by choosing those points that have higher values of multi-scale curvatures. In practice, similar to the suggestion from [12], points are gathered with the top n^{e} largest multi-scale curvatures as the feature points individually within n^{r} horizontal polar subregions for each row, where we use a lower bound to exclude feature points with low multi-scale curvatures. We denote $\mathcal{F}_t \subseteq \mathcal{X}_t$ as the set of feature points with respect to $\mathcal{R}_t$.

B. Selecting and Pruning Feature Correspondences

A pair $(\boldsymbol{x}, \boldsymbol{y}) \in \mathcal{F}_t \times \mathcal{F}_{t-1}$ is said to be an inlier point correspondence if $\|\boldsymbol{y} - R^\star \boldsymbol{x} - \boldsymbol{t}^\star\|_2 \leq \varepsilon$, where $(R^\star, \boldsymbol{t}^\star)$ is the ground truth rigid transformation between $\mathcal{X}_t$ and $\mathcal{X}_{t-1}$.

A challenge in correspondence-free scan matching is to find inlier feature correspondences between two different point clouds. To efficiently get a small number of feature point correspondences, one assumes that a correspondence $(\boldsymbol{x}, \boldsymbol{y})$ is more likely to be correct if their distance is small.

The procedure of feature matching in KCP includes two steps. In the first step, the k-closest points (k-CP) in $\mathcal{F}_{t-1}$ for each point in $\mathcal{F}_t$ are selected to be the candidate feature correspondences. Given two sets of feature points $\mathcal{F}_t$ and $\mathcal{F}_{t-1}$ calculated in Section III-A, the initial set of correspondences is defined by

$$\bar{\mathcal{C}}_{t,t-1} = \bigcup_{\boldsymbol{x} \in \mathcal{F}_t} \Big\{(\boldsymbol{x}, \boldsymbol{y}) : \boldsymbol{y} \in \mathcal{T}(\mathcal{F}_{t-1}, \boldsymbol{x}, k)\Big\}, \tag{6}$$

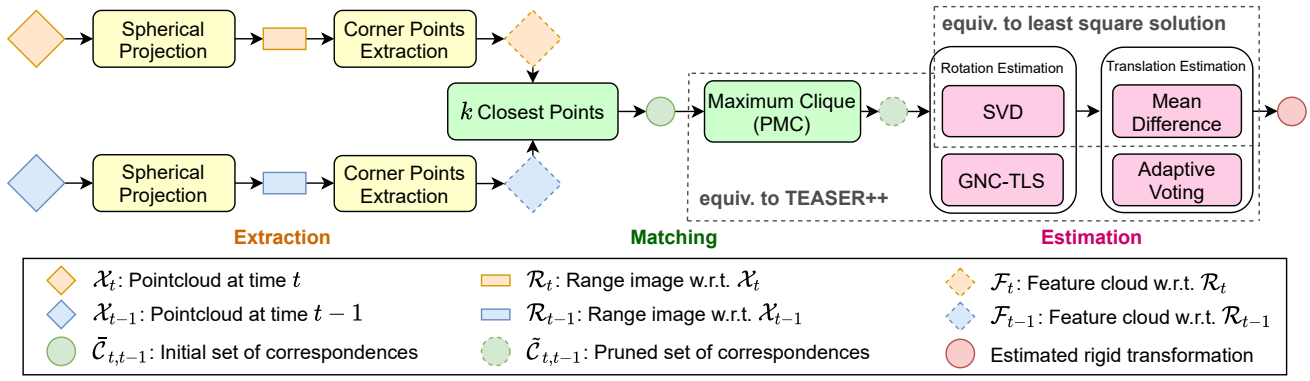

Fig. 2: System architecture of KCP. The proposed method using the least square solution is called KCP-SVD, and the proposed method using TEASER++ is called KCP-TEASER.

where $\mathcal{T}(\mathcal{F}_{t-1}, \boldsymbol{x}, k)$ is the set of k-closest points of $\boldsymbol{x}$ in $\mathcal{F}_{t-1}$, which can be obtained by using the kd-tree data structure. k is a hyper-parameter that affects the cardinality and the inlier correspondence rate of $\bar{\mathcal{C}}_{t,t-1}$ in KCP. The number of correct correspondences increases with k, but the inlier correspondence rate drops with excessive k. A desirable k is set such that $\bar{\mathcal{C}}_{t,t-1}$ has high inlier rate and low cardinality.

In the second step, $\bar{\mathcal{C}}_{t,t-1}$ is pruned to obtain a more accurate set of correspondences with graph-based pairwise constraints. This process is the same as TEASER's [9] and TEASER++'s [8], but for clarity and completeness, we provide a concise theoretical review, and newly introduce the outlier correspondence penetration issue within the derivation. The main idea is to consider the maximum clique problem on an association graph, where nodes represent feature point correspondences and edges represent consensus relationships of two correspondences [7]–[9], [24]. To construct the association graph, for any two different points $\boldsymbol{x}_1, \boldsymbol{x}_2 \in \mathcal{F}_t$, we adopts the following measures defined in [8]:

$$m^{\text{TIM}}(\boldsymbol{x}_1, \boldsymbol{x}_2) = \boldsymbol{x}_1 - \boldsymbol{x}_2, \tag{7}$$

$$m^{\text{TRIM}}(\boldsymbol{x}_1, \boldsymbol{x}_2) = \left\| m^{\text{TIM}}(\boldsymbol{x}_1, \boldsymbol{x}_2) \right\|_2, \tag{8}$$

where $m^{\text{TIM}}(\boldsymbol{x}_1, \boldsymbol{x}_2) \in \mathbb{R}^3$ is the *translation invariant measurement* (TIM) and $m^{\text{TRIM}}(\boldsymbol{x}_1, \boldsymbol{x}_2) \in \mathbb{R}_{\geq 0}$ is the *translation and rotation invariant measurement* (TRIM). We define that $(c_1, c_2) \in \bar{\mathcal{C}}_{t,t-1} \times \bar{\mathcal{C}}_{t,t-1}$ is an inlier TIM pair if

$$\left\| m^{\text{TIM}}(\boldsymbol{x}_1, \boldsymbol{x}_2) - R^\star m^{\text{TIM}}(\boldsymbol{y}_1, \boldsymbol{y}_2) \right\|_2 \leq 2\varepsilon, \tag{9}$$

and (c_1, c_2) is an inlier TRIM pair if

$$\left| m^{\text{TRIM}}(\boldsymbol{x}_1, \boldsymbol{x}_2) - m^{\text{TRIM}}(\boldsymbol{y}_1, \boldsymbol{y}_2) \right| \leq 2\varepsilon, \tag{10}$$

where $c_1 = (\boldsymbol{x}_1, \boldsymbol{y}_1)$ and $c_2 = (\boldsymbol{x}_2, \boldsymbol{y}_2)$.

Using the triangle inequality, one can obtain Lemma 1, which describes the relationship between inlier feature correspondences and inlier TRIM pairs.

Lemma 1. *Let $c_1, c_2 \in \bar{\mathcal{C}}_{t,t-1}$. If c_1 and c_2 are inlier feature correspondences, then (c_1, c_2) is an inlier* TRIM *pair.*

It is now sufficient to define the association graph by

$$\mathcal{G}_{t,t-1} = (\bar{\mathcal{C}}_{t,t-1}, \mathcal{E}_{t,t-1}), \tag{11}$$

where $\mathcal{E}_{t,t-1}$ is the set of all inlier TRIM pairs, i.e., each edge in $\mathcal{G}_{t,t-1}$ denotes one inlier TRIM pair. Then Theorem 2, similar to Theorem 6 in [8], provides a graph-based trick to estimate a subset of $\bar{\mathcal{C}}_{t,t-1}$. This subset is called *clique*, which is expected to have a higher inlier rate than $\bar{\mathcal{C}}_{t,t-1}$.

Theorem 2 (Clique for Inlier Feature Correspondences)**.** *The set of inlier feature correspondences is a clique in $\mathcal{G}_{t,t-1}$.*

Theorem 2 can be proved directly by Lemma 1. It is suggested in [8] to choose the maximum clique $\tilde{\mathcal{C}}_{t,t-1}$ of the graph $\mathcal{G}_{t,t-1}$ to obtain a pruned set of correspondences, and a parallel maximum clique algorithm (PMC) [28] is used in KCP to efficiently calculate the clique. In theoretical aspects, however, please note that the reverse of Lemma 1 does not hold. This implies that outlier feature correspondences could still be included in $\tilde{\mathcal{C}}_{t,t-1}$. Furthermore, the maximum clique $\tilde{\mathcal{C}}$ might not contain all inlier correspondences in $\bar{\mathcal{C}}$. This is a potential problem of applying maximum clique that has rarely been addressed from a theoretical point of view, and we call this problem *the outlier correspondence penetration issue*. An empirical discussion will be provided in Section IV-A.

C. Estimation of the Relative Pose

With the components described in previous subsections and the assumption $\mathcal{C}_{t,t-1} = \tilde{\mathcal{C}}_{t,t-1}$, we now can solve the optimization problem of Equation (1). We use the graduated non-convexity approach with the truncated least squares (GNC-TLS) [21] and the adaptive voting algorithm, proposed by TEASER++ [8], to estimate the relative rotation and translation respectively under the truncated least squares problem, which is able to suppress extreme costs from outlier correspondences. If there is very few outlier correspondences in $\tilde{\mathcal{C}}_{t,t-1}$, the optimization problem has a closed-form solution that can be obtained through SVD [14].

IV. Experiments

We evaluate the proposed method[1] by two LiDAR scan matching experiments, one with synthetic data, and the other

[1]Code is available at https://github.com/StephLin/KCP.

TABLE I: Experiment configuration.

Category	Parameter	Value
Point cloud	Number of channels	32
	Range of vertical FOV (deg)	$[-30.0, 10.0]$
	Lower bound z-axis value (m)	-1.5
Range image	Resolution of Horizontal FOV n^{h}	1800
	Resolution of Vertical FOV n^{v}	144
Feature points	Number of curvature scales n^{s}	5
	Horizontal polar subregions n^{r}	6
	Lower bound of multi-scale curvature	30.0
KCP	k	$\{1, 2\}$
	Noise bound (m)	0.06

with real-world nuScenes dataset [13]. Experiment configuration is listed in Table I. Point clouds used in the experiments are collected by a 32-beam spinning LiDAR sensor with 360° horizontal FOV and 20Hz capture frequency. Relative pose errors in translation (meters per frame) and rotation (degrees per frame) are used as the evaluation metrics. The success rate is also computed, where a successful registration is defined as one whose translation error is below 0.1 meters and rotation error below 0.5 degrees.

The performance of KCP-TEASER is compared with local registration methods (ICP [3], GICP [6], NDT [5]) and global registration methods (Go-ICP [4], Fast Global Registration (FGR) [29], FPFH-based TEASER++ (FPFH-TEASER) [8], 3DSmoothNet-based TEASER++ (3DSN-TEASER) [8]). We use the implementation released by the authors of each method except ICP, GICP, and NDT, which are implemented by the Point Cloud Library and Autoware. A putative set of correspondences computed using FPFH, as introduced in [8], is used as the initial guess of point correspondences for FPFH-TEASER. Referred to experiment setups of 3DSmoothNet [10], 2000 points of each point cloud are randomly chosen to match and register for 3DSN-TEASER. For input data, ICP is experimented with corner points calculated by the proposed corner points extraction method, and the other approaches are experimented with the raw point clouds. All experiments are conducted on a desktop computer with an Intel i7-8700 CPU, 16GB RAM, and a GeForce GTX 1060 6GB graphical card for computing 3DSmoothNet.

A. Synthetic LiDAR Scan Matching Experiment

In this experiment, 40 point clouds in the nuScenes dataset are randomly selected as the source point clouds. For each source point cloud, 60 random transformations are applied on the source point cloud as target point clouds, and Gaussian white noises of $0.02\mathrm{m}$ standard deviation are applied to all the points in each dimension. The sampling of the translation part follows the uniform distribution $U[-1, 1]^3$ in meter. In view of the axis-angle representation of rotation, the sampling of the axis follows the uniform distribution on the 3D unit sphere, and the sampling of the angle follows the uniform distribution $U[-10, 10]$ in degree.

Table II and Figure 3 present root-mean-square transformation errors with respect to average computational time. KCP-TEASER of $k = 2$ attains comparable RMSE accuracy with 3DSN-TEASER and GoICP, while the average computational time of KCP-TEASER is much smaller than those of 3DSN-TEASER and GoICP. On the other hand, this experiment also indicates that KCP-SVD and KCP-TEASER are more accurate than other local registration approaches, where KCP-TEASER of $k = 2$ provides a slower but more accurate transformation result than KCP-TEASER of $k = 1$.

TABLE II: Relative transformation errors and average computational time in the synthetic scan matching task.

Method	Translation (m/frame)		Rotation (deg/frame)		Time (sec/frame)	Success Rate
	Mean	RMSE	Mean	RMSE	Mean	
ICP	0.075	0.106	0.100	0.329	**0.009**	78.1%
NDT	0.033	0.042	0.111	0.160	0.390	96.8%
GICP	**0.002**	0.028	0.007	0.225	0.090	**100%**
Go-ICP	0.006	0.008	**0.004**	**0.006**	13.433	**100%**
FGR	0.093	0.115	0.817	0.925	0.532	18.8%
FPFH-TEASER	0.026	0.039	0.232	0.385	0.506	89.2%
3DSN-TEASER	0.004	**0.005**	0.010	0.011	6.327	**100%**
KCP-SVD (k=1)	0.016	0.028	0.023	0.045	0.022	98.9%
KCP-TEASER (k=1)	0.006	0.011	0.014	0.034	0.024	99.9%
KCP-TEASER (k=2)	0.005	0.006	0.012	0.014	0.049	**100%**

Ablation Study. Comparing the transformation RMSEs of ICP and KCP-SVD, we attribute the improvement to that exploiting the graph-based pairwise constraints on the correspondences set is beneficial to figure out correct correspondences instead of finding closest points iteratively. Moreover, a smaller transformation error is obtained when replacing SVD with TEASER++ of $k = 1$. This progress shows that leveraging truncated least squares is effective to obtain a more accurate transformation, but it also implies that there are still some incorrect correspondences within the maximum clique. The theoretical discussion of the problem is mentioned in Section III-B. Furthermore, since KCP-TEASER of $k = 2$ considers more feature point correspondences than the one of $k = 1$, a better estimation result is obtained by increasing k from 1 to 2, and meanwhile, due to the computation of maximum clique, a higher computational cost is borne.

To examine the range of the transformation between two scans that our registration method can withstand, we further modify the sampling method to conduct a robustness evaluation experiment consisted of two sessions. For the translation session, point clouds are not rotated but translated uniformly on $\{(rx, ry, rz) : \|(x, y, z)\| = 1\}$ with $r \in \{1, 1.5, 2, 2.5, 3\}$. As for the rotation session, point clouds are not translated but rotated with an angle randomly picked from $\{10, 15, 20, 25, 30\}$ degrees. There are 10 sampling configurations and each configuration would generate 2400 scan matching tasks. Figures 4 and 5 show the trend of registration error when the synthetic (ground truth) translation/ration increases[2]. Compared to other local registration approaches, KCP is insensitive to the increase of translation. However, KCP is relatively sensitive to the increase of rotation.

[2]For complete results, please refer to https://github.com/StephLin/KCP.

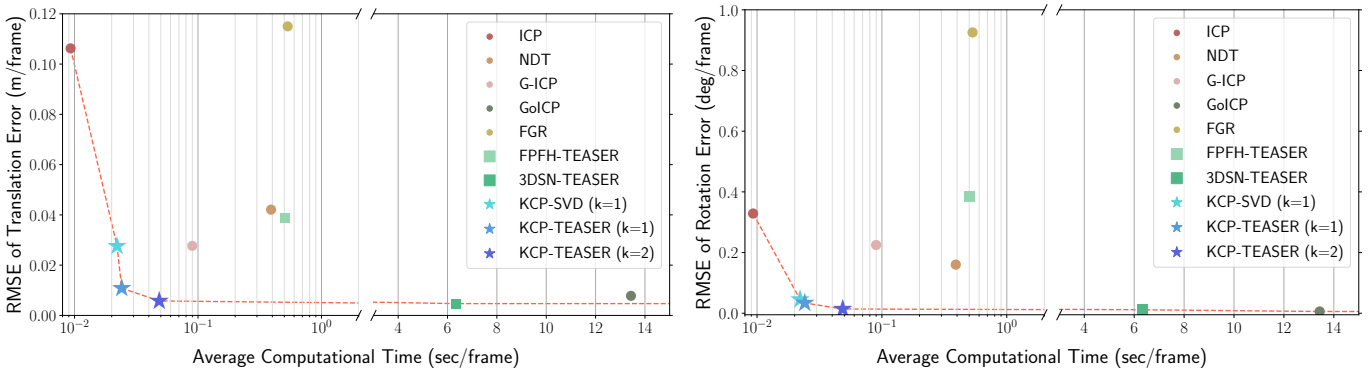

Fig. 3: Root-mean-square errors of translation (left) and rotation (right) parts with respect to average computational time in the synthetic scan matching task. Red dotted lines are lower bounds of RMSE with respect to average computational time.

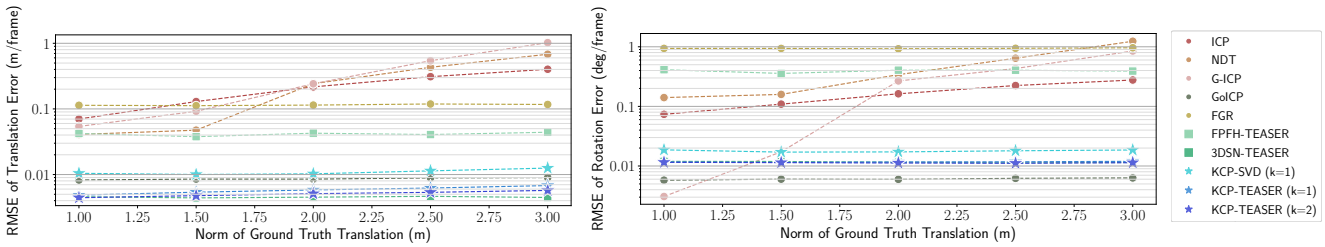

Fig. 4: Robustness test against large translation. The proposed method is robust against translation (up to 3m), which has comparable insensitivity as global registration approaches.

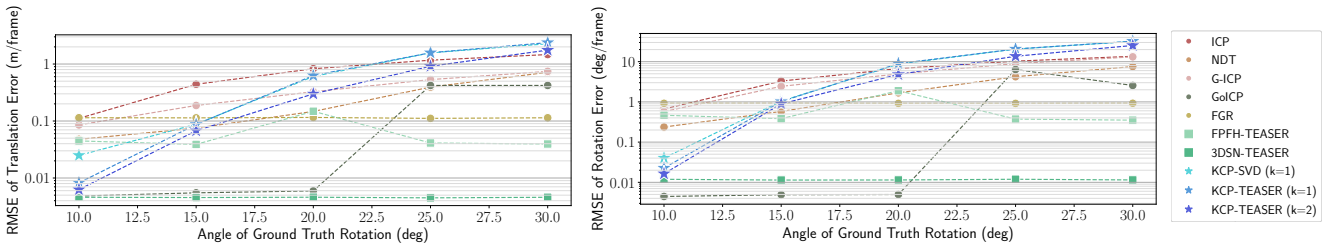

Fig. 5: Robustness test against large rotation. Compared to translation, the proposed method is relatively less robust as it can only handle rotation up to 10 degrees.

B. Real-world LiDAR Scan Matching

In this experiment, the first 48 scenes of the nuScenes dataset [13] are chosen to be the testing data, and scan matching are performed on any two consecutive LiDAR scans (18439 registrations in total) without initial guess of relative rigid transformation. The ego vehicle trajectories in the nuScenes dataset are used as the ground truth solution, where the relative transformation between two scans is up to a translation of 1.31 meters and a rotation of 2.29 degrees. Our method could achieve 99.7% success rate. Table III lists mean errors and root-mean-square errors of the relative pose, Figure 6 shows the pose errors in the form of box plot, and Figure 7 shows the computational time of each method in this experiment.

In summary, KCP considers fewer correspondences (instead of the direct product) of two point clouds, resulting in a lower cost of computing the maximum clique. Moreover, KCP searches point correspondences in a local region and avoids a complex computation of feature descriptor, at the expense of global registration feasibility. KCP-TEASER obtains a faster, more accurate, and more stable registration results than both FPFH and 3DSmoothNet based TEASER++. Experiment results also indicate that laser scan matching approaches with KCP are able to provide fast and accurate estimations in this real-world scan matching problem.

TABLE III: Relative transformation errors and average computational time in the real-world scan matching task.

Method	Translation (m/frame)		Rotation (deg/frame)		Time (sec/frame)	Success Rate
	Mean	RMSE	Mean	RMSE	Mean	
ICP	0.038	0.043	0.100	0.123	**0.015**	99.2%
NDT	0.053	0.066	0.136	0.167	0.151	89.0%
GICP	0.023	0.037	**0.073**	**0.097**	0.104	99.3%
Go-ICP	0.060	0.073	0.100	0.125	22.443	85.9%
FGR	0.054	0.068	0.237	0.272	0.867	85.7%
FPFH-TEASER	0.047	0.103	0.294	0.819	0.395	83.0%
3DSN-TEASER	0.022	0.033	0.106	0.135	6.357	99.1%
KCP-SVD (k=1)	0.020	0.022	0.104	0.128	0.023	**99.7%**
KCP-TEASER (k=1)	0.019	0.022	0.101	0.125	0.025	**99.7%**
KCP-TEASER (k=2)	**0.018**	**0.020**	0.101	0.125	0.077	**99.7%**

V. Conclusion and Future Work

We present KCP, an efficient and effective laser scan matching approach inspired from LOAM and TEASER++.

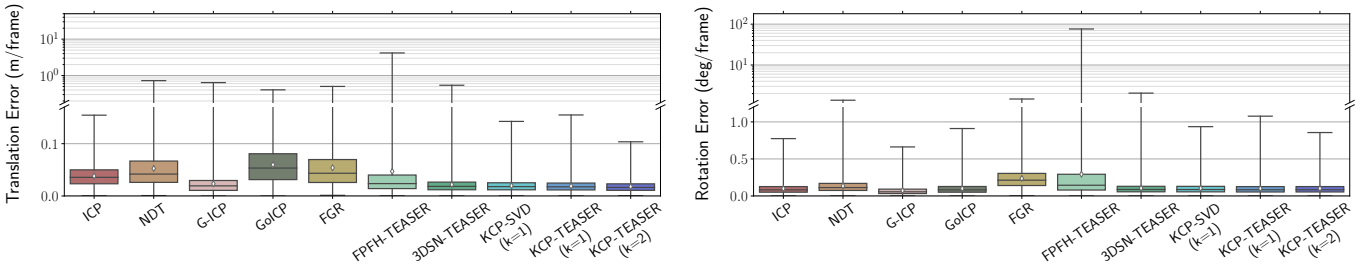

Fig. 6: Relative pose errors with respect to translation (left) and rotation (right) parts in the real-world LiDAR scan matching task. Note that figures are expressed in the type of box plot and diamond dots are corresponding mean errors.

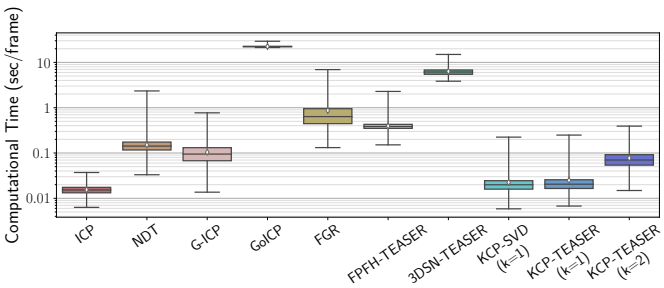

Fig. 7: Computational time of registration approaches in the real-world LiDAR scan matching experiment.

We improve the efficiency by using corner point extraction with the multi-scale curvature and using corner point matching with the k-closest points, resulting in a small number of point correspondences that can avoid the high computational cost of the maximum clique algorithm. We also enhance the effectiveness by integrating the k-closest points approach with the graph-based pairwise constraints. Our experiment results show that both KCP-SVD and KCP-TEASER achieve state-of-the-art accuracy while maintaining low computational cost. Besides, KCP-TEASER is more capable to resist incorrect correspondences than KCP-SVD.

Similar to other local registration approaches, KCP cannot provide an accurate registration when there is an extreme translation or rotation between two point clouds. We would like to extend the proposed method to a global registration approach by investigating a fast and reliable point descriptor. Besides, we also want to figure out a strategy to estimate a proper k under various registration situations. Finally, we plan to develop a distribution-based KCP to resist irregular bias within laser scans.

REFERENCES

[1] X. Huang, G. Mei, J. Zhang, and R. Abbas, "A comprehensive survey on point cloud registration," *arXiv preprint arXiv:2103.02690*, 2021.

[2] L. Bernreiter, L. Ott, J. Nieto, R. Siegwart, and C. Cadena, "PHASER: A Robust and Correspondence-Free Global Pointcloud Registration," *RA-L*, vol. 6, no. 2, pp. 855–862, 2021.

[3] P. J. Besl and N. D. McKay, "A method for registration of 3-D shapes," *TPAMI*, vol. 14, no. 2, pp. 239–256, 1992.

[4] J. Yang, H. Li, D. Campbell, and Y. Jia, "Go-ICP: A globally optimal solution to 3d ICP point-set registration," *IEEE Trans. Pattern Anal. Mach. Intell.*, vol. 38, no. 11, pp. 2241–2254, 2016.

[5] M. Magnusson, A. Lilienthal, and T. Duckett, "Scan Registration for Autonomous Mining Vehicles Using 3D-NDT," *Journal of Field Robotics*, vol. 24, no. 10, pp. 803–827, 2007.

[6] A. Segal, D. Haehnel, and S. Thrun, "Generalized-ICP," in *Robotics: Science and Systems*, vol. 2, no. 4. Seattle, WA, 2009, p. 435.

[7] Á. Parra, T.-J. Chin, F. Neumann, T. Friedrich, and M. Katzmann, "A Practical Maximum Clique Algorithm for Matching with Pairwise Constraints," *arXiv preprint arXiv:1902.01534*, 2019.

[8] H. Yang, J. Shi, and L. Carlone, "TEASER: Fast and Certifiable Point Cloud Registration," *T-RO*, vol. 37, no. 2, pp. 314–333, 2020.

[9] H. Yang and L. Carlone, "A Polynomial-time Solution for Robust Registration with Extreme Outlier Rates," in *Robotics: Science and Systems*, 2019.

[10] Z. Gojcic, C. Zhou, J. D. Wegner, and A. Wieser, "The Perfect Match: 3D Point Cloud Matching with Smoothed Densities," in *CVPR*, 2019, pp. 5545–5554.

[11] R. B. Rusu, N. Blodow, and M. Beetz, "Fast Point Feature Histograms (FPFH) for 3D Registration," in *ICRA*. IEEE, 2009, pp. 3212–3217.

[12] J. Zhang and S. Singh, "LOAM: Lidar Odometry and Mapping in Real-time," in *Robotics: Science and Systems*, 2014.

[13] H. Caesar, V. Bankiti, A. H. Lang, S. Vora, V. E. Liong, Q. Xu, A. Krishnan, Y. Pan, G. Baldan, and O. Beijbom, "nuScenes: A multimodal dataset for autonomous driving," in *CVPR*, 2020, pp. 11 621–11 631.

[14] B. Horn, H. Hilden, and S. Negahdaripour, "Closed-Form Solution of Absolute Orientation using Orthonormal Matrices," *Journal of the Optical Society of America A*, vol. 5, pp. 1127–1135, 07 1988.

[15] H. Lei, G. Jiang, and L. Quan, "Fast descriptors and correspondence propagation for robust global point cloud registration," *IEEE Transactions on Image Processing*, vol. 26, no. 8, pp. 3614–3623, 2017.

[16] Z. J. Yew and G. H. Lee, "3DFeat-Net: Weakly Supervised Local 3D Features for Point Cloud Registration," in *ECCV*, 2018, pp. 607–623.

[17] C. Choy, J. Park, and V. Koltun, "Fully Convolutional Geometric Features," in *ICCV*, 2019, pp. 8958–8966.

[18] G. Tinchev, A. Penate-Sanchez, and M. Fallon, "SKD: Keypoint Detection for Point Clouds using Saliency Estimation," *IEEE Robotics Autom. Lett.*, vol. 6, no. 2, pp. 3785–3792, 2021.

[19] X. Bai, Z. Luo, L. Zhou, H. Fu, L. Quan, and C. Tai, "D3feat: Joint learning of dense detection and description of 3d local features," in *Proc. Conf. Comput. Vis. Pattern Recognit.*, 2020, pp. 6359–6367.

[20] M. A. Fischler and R. C. Bolles, "Random sample consensus: A paradigm for model fitting with applications to image analysis and automated cartography," *Communications of the ACM*, vol. 24, no. 6, pp. 381–395, 1981.

[21] H. Yang, P. Antonante, V. Tzoumas, and L. Carlone, "Graduated Non-Convexity for Robust Spatial Perception: From Non-Minimal Solvers to Global Outlier Rejection," *RA-L*, vol. 5, no. 2, pp. 1127–1134, 2020.

[22] N. Gelfand, N. J. Mitra, L. J. Guibas, and H. Pottmann, "Robust Global Registration," in *Symposium on Geometry Processing*. Vienna, Austria, 2005, pp. 197–206.

[23] S. H. Cen and P. Newman, "Radar-only ego-motion estimation in difficult settings via graph matching," in *ICRA*, 2019, pp. 298–304.

[24] R. C. Bolles and R. A. Cain, "Recognising and Locating Partially Visible Objects: The Local-Feature-Focus Method," in *Robot Vision*. Springer, 1983, pp. 43–82.

[25] O. Enqvist, K. Josephson, and F. Kahl, "Optimal Correspondences from Pairwise Constraints," in *ICCV*, 2009, pp. 1295–1302.

[26] S. Gold, A. Rangarajan *et al.*, "Softmax to Softassign: Neural Network Algorithms for Combinatorial Optimization," *Journal of Artificial Neural Networks*, vol. 2, no. 4, pp. 381–399, 1996.

[27] C. Gonzalez and M. Adams, "An improved feature extractor for the Lidar Odometry and Mapping (LOAM) algorithm," in *ICCAIS*, 2019, pp. 1–7.

[28] R. A. Rossi, D. F. Gleich, and A. H. Gebremedhin, "Parallel maximum clique algorithms with applications to network analysis," *SIAM J. Sci. Comput.*, vol. 37, no. 5, 2015.

[29] Q.-Y. Zhou, J. Park, and V. Koltun, "Fast Global Registration," in *ECCV*, 2016, pp. 766–782.